Inorg. Chem. **2007**, *46*, 5404–5410

Controlled Hydrothermal Growth and Up-Conversion Emission of $NaLnF_4$ (Ln = Y, Dy–Yb)

Jianle Zhuang,[†] Lifang Liang,[†] Herman H. Y. Sung,[‡] Xianfeng Yang,[†] Mingmei Wu,*[,†] Ian D. Williams,[‡] Shouhua Feng,[§] and Qiang Su[†]

MOE Key Laboratory of Bioinorganic and Synthetic Chemistry, State Key Laboratory of Optoelectronic Materials and Technologies and School of Chemistry and Chemical Engineering, Sun Yat-Sen (Zhongshan) University, Guangzhou 510275, P. R. China, Department of Chemistry, Hong Kong University of Science and Technology, Clear Water Bay, Kowloon, Hong Kong, P. R. China, and State Key Laboratory of Inorganic Synthesis and Preparative Chemistry, Jilin University, Changchun 130023, P. R. China

Received February 5, 2007

The controlled hydrothermal preparation of $NaYF_4$ as both cubic and hexagonal phase types with specific associated morphologies, nanospheres and microtubes, respectively, has been achieved in the absence of organic solvents. The hexagonal $NaYF_4$ compound can be prepared in novel microtubular form and directly co-doped with Yb^{3+}/Er^{3+} ions. When excited by infrared light of 980 nm, these hexagonal $NaYF_4$ microtubes display strong green up-conversion emission, which was much more intense than that of cubic $NaYF_4$ or hexagonal $NaYF_4$ nanoparticles. Other related hexagonal-prismatic microtubes of $NaLnF_4$ (Ln = Dy–Yb) were also synthesized. A growth mechanism for the microtubes is proposed. In general, the diameter of the hexagonal $NaLnF_4$ microtubes is strongly dependent on the Ln^{3+} size and increases as the rare-earth ionic radius decreases.

Introduction

Rare-earth ion-doped fluorides based on $ALnF_4$ (A = alkaline metal, Ln = rare-earth element) have been investigated for several decades due to their electrical and optical properties and wide applications as solid electrolytes, solid-state lasers, and up- or down-conversion hosts.[1−13] Among them, most of the attention has been focused on $NaYF_4$ because it is a particularly important host material for green and blue up-conversion (UC) phosphors. It is well-established that hexagonal $NaYF_4$ is the most efficient UC host material known to date[4−7] and has great potential applications in solid-state lasers, solar cells, and biolabels.[3−13] Traditionally, $NaYF_4$ was prepared via solid-state reaction from stoichiometric mixtures of highly purified NaF and YF_3 with other

* To whom correspondence should be addressed. E-mail: ceswmm@mail.sysu.edu.cn.
† Sun Yat-Sen (Zhongshan) University.
‡ Hong Kong University of Science and Technology.
§ Jilin University.

(1) (a) Tsuboi, T.; Murayama, H.; Shimamura, K. *J. Alloys Compd.* **2006**, *408*, 776−779. (b) You, F. T.; Huang, S. H.; Liu, S. M.; Tao, Y. *J. Lumin.* **2004**, *110*, 95−99.
(2) (a) Zakaria, D.; Mahiou, R.; Avignant, D.; Zahir, M. *J. Alloys Compd.* **1997**, *257*, 65−68. (b) Wegh, R. T.; Donker, H.; Oskam, K. D.; Meijerink, A. *Science* **1999**, *283*, 663−666. (c) Zakaria, D.; Fournier, M. T.; Mahiou, R.; Cousseins, J. C. *J. Alloys Compd.* **1992**, *188*, 250−254. (d) Reddy, M. J.; Sreekanth, T.; Rao, U. V. S. *Solid State Ionics* **1999**, *126*, 55−63. (e) Wang, M.; Huang, Q. L.; Hong, J. M.; Wu, W. H.; Yu, Z.; Chen, X. T.; Xue, Z. L. *Solid State Commun.* **2005**, *136*, 210−214.
(3) (a) Liu, F.; Ma, E.; Chen, D.; Yu, Y.; Wang, Y. *J. Phys. Chem. B* **2006**, *110*, 20843−20846. (b) Chong, K. J.; Hirai, T.; Kawai, T.; Hashimoto, S.; Ohno, N. *J. Lumin.* **2007**, *122*, 149−151.
(4) (a) Kramer, K. W.; Biner, D.; Frei, G.; Gudel, H. U.; Hehlen, M. P.; Luthi, S. R. *Chem. Mater.* **2004**, *16*, 1244−1251. (b) Suyver, J. F.; Grimm, J.; van Veen, M. K.; Biner, D.; Kramer, K. W.; Gudel, H. U. *J. Lumin.* **2006**, *117*, 1−12. (c) Shalav, A.; Richards, B. S.; Trupke, T.; Kramer, K. W.; Gudel, H. U. *Appl. Phys. Lett.* **2005**, *86*, 013505. (d) Suyver, J. F.; Aebischer, A.; Biner, D.; Gerner, P.; Grimm, J.; Heer, S.; Kramer, K. W.; Reinhard, C.; Gudel, H. U. *Opt. Mater.* **2005**, *27*, 1111−1130. (e) Suyver, J. F.; Grimm, J.; Kramer, K. W.; Gudel, H. U. *J. Lumin.* **2005**, *114*, 53−59.
(5) Heer, S.; Koempe, K.; Guedel, H.-U.; Haase, M. *Adv. Mater.* **2004**, *16*, 2102−2105.
(6) Liang, L. F.; Wu, H.; Hu, H. L.; Wu, M. M.; Su, Q. *J. Alloys Compd.* **2004**, *368*, 94−100.
(7) (a) Wang, L.; Li, Y. *Chem. Commun.* **2006**, 2557−2559. (b) Wang, L. Y.; Li, Y. D. *Nano Lett.* **2006**, *6*, 1645−1649. (c) Zeng, J. H.; Su, J.; Li, Z. H.; Yan, R. X.; Li, Y. D. *Adv. Mater.* **2005**, *17*, 2119−2123.
(8) Yi, G. S.; Lu, H. C.; Zhao, S. Y.; Yue, G.; Yang, W. J.; Chen, D. P.; Guo, L. H. *Nano Lett.* **2004**, *4*, 2191−2196.
(9) (a) Boyer, J.-C.; Vetrone, F.; Cuccia, L. A.; Capobianco, J. A. *J. Am. Chem. Soc.* **2006**, *128*, 7444−7445. (b) Boyer, J.-C.; Cuccia, L. A.; Capobianco, J. A. *Nano Lett.* **2007**, *7*, 847−852. (c) Yi, G. S.; Chow, G. M. *Adv. Funct. Mater.* **2006**, *16*, 2324−2329.
(10) Mai, H. X.; Zhang, Y. W.; Si, R.; Yan, Z. G.; Sun, L. D.; You, L. P.; Yan, C. H. *J. Am. Chem. Soc.* **2006**, *128*, 6426−6436.

10.1021/ic070220e CCC: $37.00
Published on Web 05/31/2007

relevant rare-earth fluoride dopants. The reaction was carried out in a sealed tube and/or under argon or even fluoride atmospheres to ensure complete fluorination.[14] Recently, several soft chemistry approaches have been applied to the synthesis of both cubic and hexagonal $NaYF_4$ with different morphologies with varying degrees of success.[5,7−13] An early example was the preparation by Haase et al. of colloids of cubic lanthanide-doped $NaYF_4$ nanocrystals using methanol as the solvent.[5] Solvothermal conditions were employed to prepare nanorods and nanoparticles of hexagonal $NaYF_4$.[7] Hydrothermal synthesis was also carried out by Zeng et al.,[7c] but it was stated that the size and morphology were not easily controlled with poorly shaped resultant microcrystals. Although hydrothermal syntheses of $NaYF_4$ have been reported,[7c,11] detailed and systematic investigations on the controlled growth and related UC emissions have not been carried out. Wang reported the hydrothermal growth of hexagonal $NaYF_4$ as hard microprisms, but their UC emission has not been reported.[11a] Well-defined and high-quality hydrothermally synthesized hexagonal $NaYF_4$ crystals and their comparably enhanced UC emissions need to be explored. The growth of high-quality hexagonal sodium rare-earth fluoride nanocrystals has been achieved by using the thermal decomposition of lanthanide trifluoroacetate precursors over 300 °C in a mixed solvent of oleic acid/oleylamine/1-octadecene; however, this approach has the drawback of the production of toxic byproducts.[9,10]

The discovery of single-wall carbon nanotubes has stimulated considerable interest in one-dimensional (1-D) structures with hollow interiors due to their unusual mechanical properties, porosity, electronic transfer, optical emission, and wide potential applications in mechanical engineering, chemical catalysis, gas storage and separation, and optoelectronic devices.[15] To date, many materials with hollow tubular structures have been synthesized, with elemental,[16] oxide,[17] nitride,[18] chalcogenide,[19] chloride,[20] silicate,[21] and even organic examples.[22] However, there are only limited reports discussing hollow fluoride materials.[23,24] Previously, we briefly reported the hydrothermal synthesis of rare-earth metal-based $NaHoF_4$ microtubes and $NaSmF_4$ nanotubes.[24] The comparative aqueous solution growth behavior of the sodium rare-earth tetrafluoride group has yet to be investigated in depth. High-quality and well-defined tubular $NaYF_4$ crystals with strong UC emission are of great importance in materials science and engineering. Herein, we describe the controlled growth of either cubic or hexagonal $NaYF_4$ crystallites using mild hydrothermal conditions without any organic cosolvent and have extended our previous work on the syntheses for the related hexagonal $NaLnF_4$ (Ln = Sm−Yb, Y) crystallites. A new tubular microstructure has been discovered for hexagonal $NaYF_4$. The optical properties of its' Yb^{3+}/Er^{3+}-co-doped phosphor have been investigated. Syntheses for the related hexagonal $NaLnF_4$ microtubes are also described for the heavy rare earths (Ln = Dy−Yb), in which the radius of Ln^{3+} is generally smaller than that of Y^{3+}.

Experimental Section

Hydrothermal Synthesis. Aqueous solutions of sodium fluoride (NaF, AR grade) and ammonium hydrogen fluoride (NH_4HF_2, AR grade) with a molar ratio of 1.0/2.0 were mixed in a Teflon beaker to form a clear solution A. Another mixed solution B of $Ln(NO_3)_3$ (Ln = Y, La, Pr, Nd, Sm−Yb) and ethylenediamine tetraacetic acid (EDTA) was prepared in a Teflon cup. A milky suspension C was first formed when the clear solution A was added into solution B under stirring. The molar ratio of the initial reactant mixture for hydrothermal synthesis is 6.0 NH_4HF_2/3.0 NaF/1.0 $Ln(NO)_3$/0.2 EDTA/700 H_2O. The initial pH value was around 3.0. Suspension C was 70% filled in a Teflon-lined stainless steel autoclave (23 mL, Parr type) and sealed for hydrothermal crystallization at different temperatures and time periods. After the autoclave was cooled, the final powder products were washed with distilled water and dried in a desiccator at ambient temperature. Hexagonal $NaYF_4$ nanoparticles were prepared using ethanol as the solvent with the same mole ratio of initial reactants except with the absence of EDTA.

(11) (a) Wang, Z. J.; Tao, F.; Yao, L. Z.; Cai, W. L.; Li, X. G. *J. Cryst. Growth* **2006**, *290*, 296−300. (b) Yang, K. S.; Yu, C. Y.; Lu, L. P.; Li, Y.; Ye, C. H.; Zhang, X. Y. *J. Rare Earths* **2006**, *24*, 757−760. (c) Wang, D. W.; Huang, S. H.; You, F. T.; Qi, S. Q.; Fu, Y. B.; Zhang, G. B.; Xu, J. H.; Huang, Y. *J. Lumin.* **2007**, *122*−*123*, 450−452.

(12) (a) Wei, Y.; Lu, F. Q.; Zhang, X. R.; Chen, D. P. *Chem. Mater.* **2006**, *18*, 5733−5737. (b) Wei, Y.; Lu, F. Q.; Zhang, X. R.; Chen, D. P. *J. Alloys Compd.* **2007**, *427*, 333−340. (c) Li, Z. Q.; Zhang, Y. *Angew. Chem. Int. Ed.* **2006**, *45*, 7732−7735. (d) Wang, F.; Chatterjee, D. K.; Li, Z. Q.; Zhang, Y.; Fan, X. P.; Wang, M. Q. *Nanotechnology* **2006**, *17*, 5786−5791.

(13) Zeng, J. H.; Li, Z. H.; Su, J.; Wang, L. Y.; Yan, R. O.; Li, Y. D. *Nanotechnology* **2006**, *17*, 3549−3555.

(14) (a) Thoma, R. E.; Hebert, G. M.; Insley, H.; Weaver, C. F. *Inorg. Chem.* **1963**, *2*, 1005−1012. (b) Reddy, C. G.; Pandaraiah, N.; Reddy, K. N. *J. Mater. Sci. Lett.* **1988**, *7*, 1225−1228. (c) Joubert, M. F.; Linares, C.; Jacquier, B.; Cassanho, A.; Jenssen, H. P. *J. Lumin.* **1992**, *51*, 175−87.

(15) (a) Iijima. S. *Nature* **1991**, *354*, 56−58. (b) Tremel, W. *Angew. Chem. Int. Ed.* **1999**, *38*, 2175−2179. (c) Ajayan, P. M. *Chem. Rev.* **1999**, *99*, 1787−1799. (d) Tenne, R. *Angew. Chem. Int. Ed.* **2003**, *42*, 5124−5132. (e) Tasis, D.; Tagmatarchis, N.; Bianco, A.; Prato, M. *Chem. Rev.* **2006**, *106*, 1105−1136. (f) Xiong, Y. J.; Mayers, B. T.; Xia, Y. N. *Chem. Commun.* **2005**, 5013−5022. (g) Baughman, R. H.; Zakhidov, A. A.; de Heer, W. A. *Science* **2002**, *297*, 787−792.

(16) Mayers, B.; Xia, Y. N. *Adv. Mater.* **2002**, *14*, 279−282.

(17) (a) Yada, M.; Mihara, M.; Mouri, S.; Kuroki, M.; Kijima, T. *Adv. Mater.* **2002**, *14*, 309−313. (b) Sun, Y.; Fuge, G. M.; Fox, N. A.; Riley, D. J.; Ashfold, M. N. R. *Adv. Mater.* **2005**, *17*, 2477−2481. (c) Tian, Z. R. R.; Voigt, J. A.; Liu, J.; McKenzie, B.; Xu, H. F. *J. Am. Chem. Soc.* **2003**, *125*, 12384−2385. (d) Chueh, Y. L.; Chou, L. J.; Wang, Z. L. *Angew. Chem. Int. Ed.* **2006**, *45*, 7773−7778.

(18) (a) Chopra, N. G.; Luyken, R. J.; Cherrey, K.; Crespi, V. H.; Cohen, M. L.; Louie, S. G.; Zettl, A. *Science* **1995**, *269*, 966−967. (b) Wu, Q.; Hu, Z.; Wang, X. Z.; Lu, Y. N.; Chen, X.; Xu, H.; Chen, Y. *J. Am. Chem. Soc.* **2003**, *125*, 10176−10177.

(19) (a) Remskar, M.; Mrzel, A.; Skraba, Z.; Jesih, A.; Ceh, M.; Demsar, J.; Stadelmann, P.; Levy, F.; Mihailovic, D. *Science* **2001**, *292*, 479−481. (b) Rosentsveig, R.; Margolin, A.; Feldman, Y.; Popovitz-Biro, R.; Tenne, R. *Chem. Mater.* **2002**, *14*, 471−473.

(20) Hacohen, Y. R.; Grunbaum, E.; Tenne, R.; Sloan, J.; Hutchison, J. L. *Nature* **1998**, *395*, 336−337.

(21) Wang, X.; Zhuang, J.; Chen, J.; Zhou, K. B.; Li, Y. D. *Angew. Chem. Int. Ed.* **2004**, *43*, 2017−2020.

(22) Yan, D. Y.; Zhou, Y. F.; Hou, J. *Science* **2004**, *303*, 65−67.

(23) (a) Wang, X.; Li, Y. D. *Angew. Chem. Int. Ed.* **2003**, *42*, 3497−3500. (b) Liang, X.; Wang, X.; Wang, L. Y.; Yan, R. X.; Peng, Q; Li, Y. D. *Eur. J. Inorg. Chem.* **2006**, *11*, 2186−2191.

(24) Liang, L. F.; Xu, H. F.; Su, Q.; Konishi, H.; Jiang, Y. B.; Wu, M. M.; Wang, Y. F.; Xia, D. Y. *Inorg. Chem.* **2004**, *43*, 1594−1596.

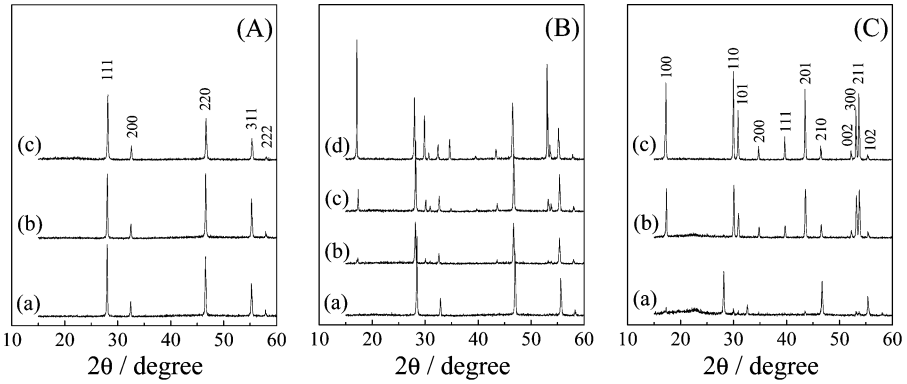

Figure 1. PXRD patterns of $NaYF_4$ synthesized (A) at 60 °C for (a) 3.0 h, (b) 24 h, and (c) 48 h; (B) at 140 °C for (a) 18 h, (b) 24 h, (c) 36 h, and (d) 48 h; (C) at 220 °C for (a) 1.0 h, (b) 3.0 h, and (c) 48 h.

Characterization. The products were characterized by using powder X-ray diffraction (PXRD) with a Philips Model PW1830 diffractometer using Cu Kα radiation ($\lambda = 0.1541$ nm) and a graphite monochromator operating at 40 kV and 30 mA with a 2θ scanning rate of $0.05°\ s^{-1}$. The sizes and shapes of particles were obtained by using a JEOL JSM-6330F field emission gun scanning electron microscope. Dried samples for scanning electron microscopy (SEM) were placed on glass-slide surfaces and then sputter-coated with platinum. Transmission electron microscopy (TEM) and selected-area electron diffraction (SAED) analyses were performed on a JEOL 2010 high-resolution transmission electron microscope equipped with an Oxford Instrument EDS system.

Infrared-to-visible UC spectra of $NaYF_4$:Yb^{3+}/Er^{3+} were recorded by exciting the sample with an unfocused beam from a 980 nm diode laser. The laser power for excitation was fixed at 45 mW for each sample for comparison of their emission intensities. The visible emissions were collected and detected by a fluorescence spectrophotometer F-4500 (Hitachi) equipped with a mechanically ruled concave diffraction grating and a R3788 photomultiplier tube.

Results and Discussion

Phase-Selective Hydrothermal Preparation of $NaYF_4$. Both cubic and hexagonal forms of $NaYF_4$ can be readily formed phase-pure under appropriate conditions. The PXRD patterns of $NaYF_4$ products synthesized at 60, 140, and 220 °C for periods between 1 and 48 h are shown in Figure 1. Subhydrothermally at 60 °C, cubic $NaYF_4$ with fluorite-related structure (JCPDF No. 77-2042) remains as the phase-pure product for reactions even up to 48 h (Figure 1A). Hydrothermal reaction at 140 °C for shorter time periods also gives cubic $NaYF_4$, but after 48 h a mixture of cubic and hexagonal phases is observed (Figure 1B). At 220 °C, the cubic form is found after 1 h but is replaced by phase-pure hexagonal $NaYF_4$ after only 3 h of reaction time. The above results indicate that there is a "phase transformation" from cubic to hexagonal $NaYF_4$ under hydrothermal conditions and that the cubic phase is a kinetic product. This is consistent with previous data that indicates that the cubic phase is thermally meta-stable up to 691 °C with respect to the hexagonal one.[14a,25] Hydrothermal synthesis with sufficiently high temperature or aging time is thus a simple, fast, and economic way to synthesize the phase-pure hexagonal form of $NaYF_4$.

(25) Thoma, R. E.; Insley, H.; Hebert, G. M. *Inorg. Chem.* **1966**, *5*, 1222−1229.

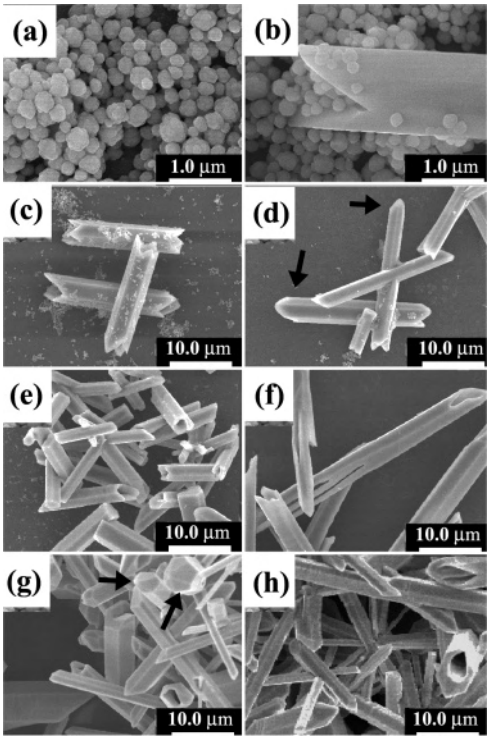

Figure 2. SEM images of $NaYF_4$ hydrothermally synthesized in the presence of EDTA at 140 °C for (a) 15 h, (b) 24 h, (c) 48 h, (d) 72 h, at 220 °C for (e) 48 h, and (f) in the absence of EDTA at 220 °C for 48 h; and SEM images of (g) $NaErF_4$ and (h) $NaYbF_4$ hydrothermally synthesized in the presence of EDTA at 220 °C for 48 h.

Hexagonal-Prismatic Microtubes and Morphological Changes of $NaYF_4$. Morphological characterization of the hydrothermally prepared $NaYF_4$ products was carried out by SEM, and selected results are shown in Figure 2. The cubic $NaYF_4$ form is found as nanospheres with an average size of around 200 nm, and this morphology persists no matter what the aging conditions. An example is shown in Figure 2a. The hexagonal $NaYF_4$ is found as hollow hexagonal-prismatic microtubes both at 140 and 220 °C (Figure 2b−f). The outer diameters of these tubes on average are around 3.0 μm, and their lengths are in the range of 10−30 μm.

The use of the EDTA additive can lead these microtubes to have better defined hexagonal tubular shape (Figure 2c−e), due to its complexing to rare-earth ions and, consequently, its modulation of the crystal growth. In the absence of EDTA, each tube of these complex fluorides became less defined

in shape and some crevices appeared along the growth directions as indicated in Figure 2f.

The crystalline structures of both nanospheres and microtubes were further characterized by electron microscopy (Supporting Information, Figure 1). The bright-field TEM images show that the cubic $NaYF_4$ product consisted of granular particles (Supporting Information, Figure 1a,b). The high-resolution TEM (HRTEM) image with the lattice fringes of 0.19 nm corresponding to (220) lattice planes of cubic $NaYF_4$ (Supporting Information, Figure 1c) and the SAED patters taken from different zone axes (Supporting Information, Figure 1d−f) indicate that these nanospheres are attributed to cubic $NaYF_4$. Whereas the HRTEM image with the lattice fringes of 0.51 nm (Supporting Information, Figure 1h) corresponding to (100) lattice planes of hexagonal $NaYF_4$ and the related SAED pattern (Supporting Information, Figure 1i) reveals the growth of the hexagonal $NaYF_4$ tube is along the *c* direction. Thus, it can be confirmed that the spherical crystals belong to cubic $NaYF_4$ and 1-D tubular microcrystals belong to hexagonal $NaYF_4$, even in a mixed phase (Supporting Information, Figure 1g,h). The diffraction results indicated that no mixed cubic−hexagonal crystalline zones were ever co-present. This implies that cubic $NaYF_4$ crystals with spherical shape are formed at the initial stage of the hydrothermal synthesis. Further hydrothermal aging then causes these spherical $NaYF_4$ crystals to dissolve and then reprecipitate separately as pure hexagonal microtubular $NaYF_4$.

Infrared-to-Visible UC of Hydrothermally Synthesized $NaYF_4$:Yb^{3+}/Er^{3+} Microtubes. Besides the facile phase-pure preparation of both cubic and hexagonal $NaYF_4$ mentioned above, the hydrothermal method also allows the ready introduction of other rare-earth dopants to act as activators or sensitizers for luminescent applications. Thus, various co-additions of Yb^{3+} and Er^{3+} into both cubic and hexagonal $NaYF_4$ have been successfully accomplished, through keeping the whole molar ratio of $Ln(NO_3)_3$ at 1.00, where Ln = Y + Yb + Er.

The mechanism for frequency up-conversion (UC) of $NaYF_4$:Yb^{3+}/Er^{3+} has been well established.[4−7] The optimum wavelength of pumping light for UC is 980 nm, which matches the $^2F_{7/2} \rightarrow {}^2F_{5/2}$ transition of the Yb^{3+} ion. The excited state $^2F_{5/2}$ of the Yb^{3+} ion may then transfer the energy to an Er^{3+} ion and populate the $^4I_{11/2}$ level. Further energy transfer from Yb^{3+} from a second photon absorption can then further excite the Er^{3+} ion from its $^4I_{11/2}$ level to $^4F_{7/2}$. Nonradiative decays from Er^{3+} $^4F_{7/2}$ to the $^2H_{11/2}$ and $^4S_{3/2}$ levels are then believed to occur. Subsequent transitions from $^2H_{11/2}$ and $^4S_{3/2}$ to the Er^{3+} ground state $^4I_{15/2}$ yield bright-green emissions at 545 and 525 nm, respectively, whereas the red emission around 660 nm is from the Er^{3+} electronic transition $^4F_{9/2} \rightarrow {}^4I_{15/2}$ (Figure 3).

Under the pumping of a 980 nm diode laser at 45 mW, Yb^{3+} and Er^{3+} co-doped hexagonal $NaYF_4$ exhibits considerably stronger emission than a similarly co-doped cubic $NaYF_4$ (Figure 3). The UC emission previously reported for the hexagonal phase is 5−10 times that of the corresponding cubic $NaYF_4$.[4a] In our work we find a ca. 20 times increase

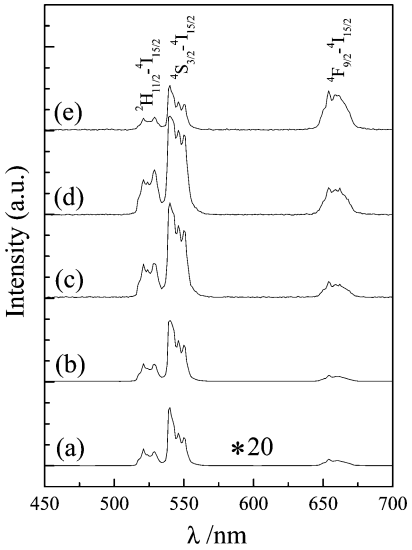

Figure 3. UC emission spectra of $NaYF_4$:Yb^{3+}/Er^{3+} excited by a 980 nm laser: (a) cubic $NaY_{0.94}Yb_{0.05}Er_{0.01}F_4$, (b) hexagonal $NaY_{0.94}Yb_{0.05}Er_{0.01}F_4$, (c) hexagonal $NaY_{0.79}Yb_{0.20}Er_{0.01}F_4$, (d) hexagonal $NaY_{0.78}Yb_{0.20}Er_{0.02}F_4$, and (e) hexagonal $NaY_{0.48}Yb_{0.50}Er_{0.02}F_4$.

for the hexagonal form compared with the cubic form measured under conditions of identical laser power density. The variable increase of the UC efficiency of hexagonal as compared with the cubic phase found in various publications may result from the different growth conditions and crystal sizes.

The change of doping concentrations of an activator and/or a sensitizer can modulate the emission intensity of each color. At low concentrations of Er^{3+}, we find that the green emission is dominant; however, the red emission becomes increasingly significant as concentrations of Er^{3+} and/or Yb^{3+} go up (Figure 3b−e). Much higher dopant concentrations result in much weaker green emission due to concentration quenching. The optimal composition for green emission from our hydrothermal-synthesized hexagonal-$NaYF_4$ host is $NaY_{0.79-0.78}Yb_{0.20}Er_{0.01-0.02}F_4$ (Figure 3). This result is qualitatively similar to those of some other reports.[5,7c] Importantly, our luminescent results confirm that an efficient co-doping of Yb^{3+} and Er^{3+} into the $NaYF_4$ host can be carried out by using a facile hydrothermal route.

Recently, hexagonal $NaYF_4$ nanoparticles were fabricated by Zeng et al. using ethanol as the solvent.[7c] We similarly prepared the hexagonal $NaYF_4$:Yb^{3+}/Er^{3+} nanoparticles (Supporting Information, Figure 2) to compare their UC emission intensity to our hexagonal microtubes obtained from hydrothermal synthesis. The UC emission of these hexagonal $NaYF_4$ nanoparticles is shown in Figure 4 and is about 4 times weaker than that of similarly doped microtubes. The result is in contrast with the previous work,[7c] which indicated the UC emission intensity of the nanoparticles is just a little weaker than that of those synthesized hydrothermally. The marked decrease of the intensity may be due to surface-quenching nanosize effect. Further studies into the differing luminescent properties of these nanoparticulate and microtubular fluorides are under investigation.

Interestingly, although the addition of EDTA in the hydrothermal reaction was found to lead to more regular

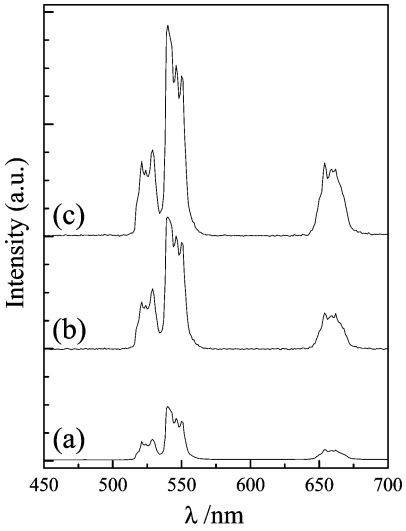

Figure 4. UC emission spectra of $NaYF_4$:Yb^{3+}/Er^{3+} excited by a 980 nm laser: (a) hexagonal nanoparticles synthesized using ethanol as the solvent, (b) hexagonal microtubes hydrothermally synthesized in the presence of EDTA, and (c) hexagonal microtubes hydrothermally synthesized in the absence of EDTA.

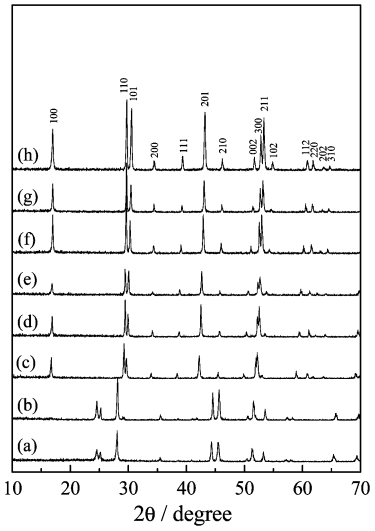

Figure 5. PXRD patterns of hydrothermal products in the system of NaF−LnF_3 (Ln = (a) Pr, (b) Nd, (c) Sm, (d) Eu, (e) Gd, (f) Tb, (g) Dy, and (h) Ho) at 140 °C for 14 h.

morphology of the hexagonal microtubes, the effect on UC efficiencies was a substantial decrease in UC emission (Figure 4). The grown crystals might adsorb some organic molecules and/or ions on the surface, and hence, their UC emission intensities are decreased due to faster nonradiative decay. We find that hexagonal $NaYF_4$ microtubes grown in the absence of EDTA display more intense UC emission than those grown in the presence of EDTA, indicating our synthetic route could make much more efficient hexagonal $NaYF_4$-based UC crystals.

Related Sodium Rare-Earth Tetrafluorides. While hexagonal $NaLnF_4$ (Ln = La−Lu, Y) compounds have been prepared for all lanthanides by solid-state reactions,[14a,25] with our hydrothermal method, hexagonal $NaLnF_4$ could not be prepared for the early lanthanide ions in the system of NaF−LnF_3 (Ln = La−Nd), with only hexagonal LnF_3 obtained instead (Figure 5a,b). Hexagonal $NaLnF_4$ has been synthesized hydrothermally in the present work with Ln = Sm−Yb (Figures 5c−h and 6c,d). The failed hydrothermal synthesis of $NaLnF_4$ (Ln = La−Nd) may be due to the relative thermodynamic stability of the hexagonal LnF_3 (Ln = La−Nd), while LnF_3 (Ln = Sm−Yb) occurs in the orthorhombic form.[25] Some reports of the synthesis of early $NaLnF_4$ phases have appeared; Mai et al. reported that $NaPrF_4$ and $NaNdF_4$ nanocrystals can be prepared in organic solvent at much higher temperatures from toxic precursors.[10] In addition, preparation of $NaCeF_4$ was previously claimed from "*basic*" organic solvent, but no detailed reactant receipts and synthesis procedures were described and we have been unsuccessful in duplicating these results.[13]

PXRD patterns of hexagonal $NaLnF_4$ (Ln = Sm−Yb) show almost identical features, indicating that these complex fluorides are isostructural. The general shift of diffraction peaks to high 2θ angle from $NaSmF_4$ to $NaHoF_4$ in Figure 5c−h and from $NaErF_4$ to $NaYbF_4$ in Figure 6c,d is due to the smaller lanthanide ionic radius as the series is traversed.

An advantage of using middle lanthanides in the hydrothermal synthesis is that phase-pure hexagonal $NaLnF_4$ (Ln = Sm−Ho) can be prepared relatively easily under mild conditions (Figure 5c−h), whereas $NaYF_4$ requires more forcing conditions as described above (Figure 1). This trend is similar to the work by Zhang and Yan[10] but contrasts that of Li.[13] Phase-pure hexagonal $NaYF_4$ can be prepared at a higher temperature and/or for a longer time, such as at 220 °C for 3.0 h (Figure 1). However, phase-pure hexagonal $NaLnF_4$ of smaller lanthanides (Ln = Er, Tm, Yb) cannot be successfully synthesized with similar condition (Figure 6b). From these PXRD patterns in Figures 1, 5, and 6, it can be interpreted that there are common properties among $NaHoF_4$, $NaYF_4$, and $NaErF_4$. Compared with the diffraction peaks of the cubic 111, the peaks of the hexagonal 110 tend to be weaker from $NaErF_4$ to $NaYbF_4$ in Figure 6b. This experimental evidence indicates that a higher temperature and/or a longer reaction time is required to prepare phase-pure hexagonal $NaLnF_4$ with a smaller Ln^{3+} ionic radius. That is, the Arrhenius activation energy (E_a) for the phase-change rate from cubic to hexagonal forms increases.[10] This result is similar to that of ref 10, in which shows that the growth of a hexagonal $NaLnF_4$ phase is strongly dependent on the Ln^{3+} size. However, hexagonal $NaLnF_4$ (Ln = Dy−Yb, Y) tends to form tubular crystals in our result but platelike crystals in ref 10.

The diameters of the $NaErF_4$ and $NaYF_4$ microtubes cannot be easily distinguished from each other in Figure 2, but they are larger than those of $NaHoF_4$ illustrated in the Supporting Information, Figure 3a,b. The diameters of $NaHoF_4$ microtubes (Supporting Information, Figure 3a,b) are generally greater than those of $NaDyF_4$ (Supporting Information, Figure 4d). Solid nanorods rather than hollow tubules are found for $NaLnF_4$ (Ln = Eu, Gd, Tb) systems (Supporting Information, Figure 4a−c). The nanorods are often jointed with X-shaped or dendritic nanostructures. We conclude by stating that the diameters of the 1-D crystals are inversely correlated with the Ln^{3+} ionic radii. In general, the microtube diameter

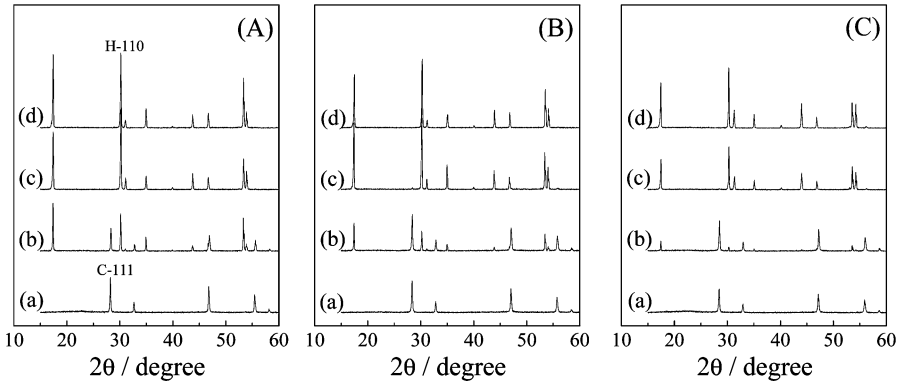

Figure 6. PXRD patterns of (A) $NaErF_3$, (B) $NaTmF_4$, and (C) $NaYbF_4$ synthesized at 220 °C for various durations: (a) 1.0 h, (b) 3.0 h, (c) 12 h, and (d) 48 h.

increases as the ionic radii of the rare-earth atoms decrease. These 1-D tubular microstructures and X-shaped nanostructures are destroyed eventually if these hydrothermal reactions are performed at much higher temperatures and/or for much longer times (typical results illustrated in Supporting Information Figure 5). In these SEM images, some grains attributed to hexagonal phases are found. This is due to the known Ostwald ripening process.

Growth Mechanism. HRTEM and SAED techniques do not indicate the presence of $NaLnF_4$ grains composed of both cubic and hexagonal structures. This suggests that the "phase transformation" is not based on an epitaxial or topotaxial growth from cubic phase to the hexagonal phase. Rather, the hydrothermal phase transformation is based on the dissolution of solid (S) crystals of cubic $NaYF_4$, the mass transfer in liquid (L) solution, and the nucleation and growth of solid crystals of hexagonal phase via a SLS (solid−liquid−solid) or a dissolution−recrystallization process; where the crystal's size of cubic $NaYF_4$ is smaller than a critical size, the cubic crystal then dissolves quickly. The sudden increase of the growth species concentrations in aqueous solution from the quick dissolution of cubic $NaYF_4$ promotes hexagonal $NaYF_4$ to grow quickly at the initial stage (Figure 2). The further redissolution of spherical grains of cubic $NaYF_4$ still serves as the component source for the maintenance of a high concentration for the further growth of the hexagonal phase with a 1-D tubular microstructure along the *c* axis during hydrothermal aging.

In Supporting Information Figure 3b, a neck is found, as pointed out by a black arrow. The connections from which the nanorods of $NaEuF_4$, $NdGdF_4$, and $NaTbF_4$ grew from and yielded X-shaped crystals were clearly observed using TEM (Supporting Information, Figure 4 (black arrows)). A bowtie-like crystal was also observed for $NaDyF_4$ (Supporting Information, Figure 4d). These findings lead us to propose that the preferential growth at the circumferential edges of these 1-D crystals (Figure 2b−h and Supporting Information Figure 3) facilitates the growth of hollow interiors in a similar way to the elongated growth of tellurium nanotubes along the $+c$ and $-c$ directions.[16] With the disappearance of spherical crystals, the growth species concentration decreases and further growth is restrained. By the maintenance of solution saturation, the further hydrothermal aging results in a pyramidal-end-capped microtube (Figure 2d,g, arrows). The further hydrothermal aging, especially performed at higher temperatures, certainly destroys these 1-D and/or hollow structures because of their intrinsic morphological metastability (Supporting Information, Figure 5).

Conclusions

In this paper, we have described a new group of well-defined prismatic microtubes based on multicomponent fluorides, typically, sodium yttrium fluoride ($NaYF_4$) by a simple hydrothermal processing from NaF, NH_4HF_2, and lanthanide nitrate. Cubic $NaYF_4$ with fluorite-related structure, the metastable phase below 691 °C, is formed as the kinetic product but is replaced by thermodynamically stable hexagonal $NaYF_4$ under hydrothermal conditions. Higher aging temperatures and/or longer aging times can promote this hydrothermal "phase transformation". Over a wide range of reaction temperatures and times, the hydrothermal route can successfully lead to an easily controlled synthesis of both cubic-phase nanospheres and hexagonal-phase microtubes of $NaYF_4$. The crystal morphology of $NaYF_4$ can be designed through consequent phase control via such wet chemistry.

Rare-earth ions such as Yb^{3+} and Er^{3+} acting as sensitizers and activators can be directly doped into both cubic and hexagonal $NaYF_4$ hosts through hydrothermal synthesis. These doped materials retain their morphologies related to their respective hosts. The hexagonal $NaYF_4$:Yb^{3+}/Er^{3+} microtubes display considerably stronger UC emission than cubic $NaYF_4$:Yb^{3+}/Er^{3+} nanospheres and hexagonal $NaYF_4$:Yb^{3+}/Er^{3+} nanoparticles. The addition of EDTA decreases the UC emission, though it makes the perfect hexagonal form.

Hydrothermal synthesis of the related sodium rare-earth fluorides is crucially dependent on the ionic radius of the rare-earth ions. In addition to $NaYF_4$, tubular $NaLnF_4$ (Ln = Dy−Yb) can be also synthesized with hollow interiors. These prismatic hollow structures are synthesized from safe and simple inorganic reactants. They can be doped with rare-earth ions hydrothermally and might be promising high-efficiency luminescence materials. As these complex fluorides generally also possess excellent fluorine-ionic conductivities, these 1-D microtubes may find wide applications as

microprobes in galvanic chemical sensors in which the hollow interiors can be designed as either anodes or cathodes.

Acknowledgment. This work is supported by the NSF of China (No. 20571087), the NSF of Guangdong (No. 5003273) for the preparation and luminescence properties of $NaYF_4$, and the State Key Laboratory of Inorganic Synthesis and Preparative Chemistry in Jilin University for rare-earth fluorides. We are indebted to Dr. Xiaoxia Zhang and Prof. Kok Wai Cheah in the Center for Advanced Luminescent Materials, Department of Physics, Hong Kong Baptist University, as well as Dr. Guokui Liu in the Chemistry Division of the Argonne National Laboratory for their helpful discussions and measurements in UC.

Note Added after ASAP Publication. This article was posted ASAP on May 31, 2007. Revised Supporting Information was added and the correct version was posted on June 7, 2007.

Supporting Information Available: Additional figures in a PDF file. This material is available free of charge via the Internet at http://pubs.acs.org.

IC070220E